ELSEVIER

Clinical Neurophysiology 110 (1999) 1793–1800

www.elsevier.nl/locate/clinph

# Using multi-stimulus VEP source localization to obtain a retinotopic map of human primary visual cortex

Scott D. Slotnick[a,*], Stanley A. Klein[b], Thom Carney[b,c], Erich Sutter[d], Shahram Dastmalchi[b]

[a]*Johns Hopkins University, Baltimore, MD, USA*
[b]*University of California at Berkeley, School of Optometry, Berkeley, CA, USA*
[c]*Neurometrics Institute, Berkeley, CA, USA*
[d]*Smith-Kettlewell Eye Research Institute, San Francisco, CA, USA*

Accepted 11 May 1999

**Abstract**

**Objective**: The goal of this study was to acquire a detailed spatial and temporal map of primary visual cortex using a novel VEP stimulus and analysis technique.

**Methods**: A multi-stimulus array spanning the central 18 degrees of the visual field was used where each of 60 checkerboard stimulus 'patches' was simultaneously modulated with an independent binary m-sequence (Sutter, 1992). VEPs corresponding to each patch were recorded from 3 subjects using a dense posterior electrode array. For each stimulus patch, single dipole source localization was conducted to determine the location, magnitude, and time-function of the underlying neural activation. To reduce ambiguity in the solution, a common time-function was assumed for stimulus patches at the same visual eccentricity (defining an annulus). The analysis was conducted independently for each annulus composed of 4–12 patches.

**Results**: The loci of the dipole solutions followed a smooth retinotopic pattern across annuli consistent with the classical organization of primary visual cortex. Specifically, each dipole was found contralateral to the corresponding stimulus patch and field inversion was observed for all subjects.

**Conclusions**: Using this technique, the most detailed spatial and temporal retinotopic map of primary visual cortex to date has been obtained. 

*Keywords:* Retinotopy; Retinotopic map; Visual-evoked potential; Multi-electrode recording; Dipole source localization; M-sequence; White noise

## 1. Introduction

Course retinotopic maps of V1 have been obtained by correlating brain lesion locations with visual field deficits (Holmes, 1945; Spalding, 1952; Horton and Hoyt, 1991a). Such studies have shown that an inverted representation of each visual hemifield maps onto the contralateral occipital cortex. The center of the visual field is bilaterally represented on the occipital pole with increasing field eccentricities projecting more anteriorly in the brain.

Detailed retinotopic maps of primary visual cortex have been obtained using functional magnetic resonant imaging (fMRI) (Sereno et al., 1994; DeYoe et al., 1996; Engel et al., 1997). These studies correlate stimulus positions in the visual field with loci of neural activation in the cortex. Although fMRI provides excellent spatial resolution, its dependence upon the hemodynamic response limits its temporal resolution and relies on assumptions regarding the relation between neural activation and the measured response.

To address the temporal limitations of fMRI, techniques can be used which depend directly on neural activity such as visual evoked potential (VEP) and magnetoencephalography (MEG) recording. Gevins (1996) stimulated the central two degrees of the visual field using sequentially presented reversing checkerboard octants and conducted VEP source localization. Dipole locations roughly matched the known contralateral and inverted retinotopic organization of primary visual cortex. Aine et al. (1996) conducted MEG source localization to 7 sequentially presented sinusoidal stimuli in the lower right quadrant of the visual field. Again, the solutions matched the classical retinotopic map of V1 reasonably well. Because each stimulus must be presented enough times to elicit a measurable response,

* Corresponding author. Department of Psychology, John Hopkins University, 3400 North Charles Street, Baltimore, MD 21218-2685, USA. Tel.: + 1-410-516-7055; fax: + 1-410-516-4478.
*E-mail address:* slotnick@adage.berkeley.edu, (S.D. Slotnick)

1388-2457/99/$ - see front matter 
CLINPH 98117
PII: S1388-2457(99)00135-2

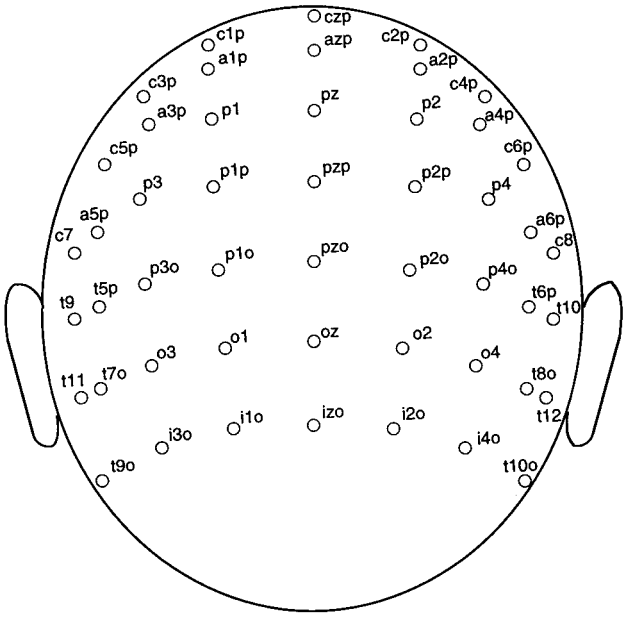


Fig. 1. Multi-electrode array used to record VEPs. Although all electrodes are approximately equidistant, those around the perimeter appear closer together due to the curvature of the head. The electrodes were imbedded in a nylon cap to ensure fast and repeatable electrode placement. All electrode impedances were maintained below 5 kΩ and electrode czp was used as a reference.

standard VEP and MEG methods are limited in the number of stimulus locations that can be used for retinotopic mapping. To overcome this limitation, we used a new method for acquiring VEPs to multiple stimulus locations simultaneously.

To determine the temporal and spatial dynamics of human visual area V1, neural responses generated by stimuli at numerous positions in the visual field must be acquired using a method with sufficient temporal resolution. We have combined two proven techniques to achieve this goal: a multi-stimulus array consisting of 60 stimulus positions (Baseler et al., 1994; Baseler and Sutter, 1997) and multi-electrode VEP dipole source localization.

## 2. Materials and methods

### 2.1. Participants

Three healthy adults (2 males, 1 female) between the ages of 28 and 48 participated in this study. All participants volunteered to take part in the study and had either normal or corrected to normal vision.

### 2.2. Electrode placement

Given our interest in V1, which is located in the posterior of the brain, an array of 43 (for subject TC) or 48 (for subjects HB and SD) electrodes was placed on the back of the head. This array included the posterior 10–20 positions (Jasper, 1958) with interpolated electrode placement to increase spatial sampling. The full array of electrodes is illustrated in Fig. 1.

### 2.3. Multi-stimulus array

The multi-stimulus array shown in Fig. 2 was used to stimulate 60 positions across the central 18° of the visual field. Subjects viewed the stimulus array binocularly.

Each checkerboard patch was simultaneously modulated with a shifted binary m-sequence (Sutter, 1992; Baseler et al., 1994) and was scaled by the cortical magnification factor of the primary visual area (Horton and Hoyt, 1991a). When using the checkerboard stimulus, the first slice of the second order kernel is analogous to the pattern reversal VEP (Baseler et al., 1994).

The m-sequence length was $2^{16}$-1 corresponding to the presentation of 65 535 stimulus frames. In this process, each patch was stimulated with 32 768 check reversals. This large number of reversals contributes to a high signal-to-noise ratio in the VEP. The frame rate was 75 Hz. Differences in timing from the top to the bottom of the screen due to the raster scan was taken into account when computing the responses to each stimulus patch (Sutter and Tran, 1992). The m-sequence was broken up into 16, 55 second data collection segments. Subjects were allowed to relax between each segment. Four to 6 sets (each consisting of the 16 segments) were averaged together for each participant. Amplifiers were set to a gain of 100 000 with a bandpass setting of 0.5–100 Hz. Electrode voltages were sampled every 1.67 ms (8 samples per video frame).

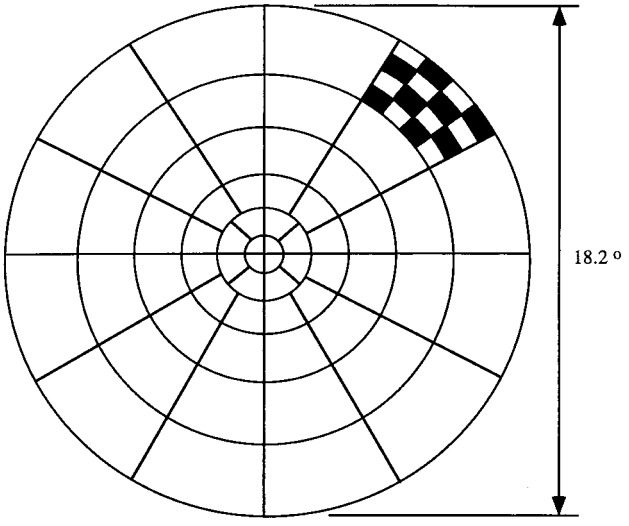


Fig. 2. Multi-stimulus array used to stimulate 60 positions across the visual field. All patches were modulated independently with a checkerboard stimulus as shown in the upper right quadrant. Baseler and Sutter (1997) used an identical stimulus array to record from a bipolar electrode configuration. Their study showed the reversal of each patch with a 4 × 4 checks/patch pattern resulted in robust electrode responses.

### 2.4. Source localization

Nearly all source localization procedures utilize the same basic framework (Scherg and Berg, 1991). Given a topographic voltage distribution, $V_{real}$ ($e$, $t$, $p$), across an electrode array $e$, over time $t$, due to a stimulus patch $p$, the goal is to find the corresponding location and time course of the underlying cortical activity that accounts for $V_{real}$. The solution is obtained by using an iterative procedure. Fig. 3 displays the method used to conduct source localization assuming one active brain region. This assumption is reasonable, since the small reversing checks with high reversal rates predominantly activate one cortical region. The 75 Hz rate of stimulation results in a mean reversal rate of 37.5 Hz for each stimulus patch. Other studies have shown that stimulation of patch reversals at high flicker rates preferentially activate primary visual cortex (Skalej et al., 1995; Schiefer et al., 1996, 1998). For each iteration, the scalp voltage ($V_{fit}$) is predicted by the model which assumes the head is a homogeneous sphere and cortical activity is a single dipole current source. The dipole moment, $\boldsymbol{M}$, describes the variation in source magnitude over time for each patch. For a given patch, the voltage distribution across an electrode position array $\boldsymbol{e}$, generated by a source at location, $\boldsymbol{r}(p)$, and moment, $\boldsymbol{M}(p, t)$, can be calculated using the formula

$$V_{fit}(\boldsymbol{e},p,t) = \boldsymbol{W}(\boldsymbol{e},\boldsymbol{r}(p))\cdot\boldsymbol{M}(p,t) \quad (1)$$

where $p$ is the patch index, $t$ is the time index, $\cdot$ indicates the dot product, and $\boldsymbol{W}$ is the Brody vector weight given by

$$\mathbf{W} = \left[\boldsymbol{e} + 2(\boldsymbol{e}-\boldsymbol{r})/d^2 + (\boldsymbol{e}(\boldsymbol{e}\cdot\boldsymbol{r}) - r)/(d + 1 - \boldsymbol{e}\cdot\boldsymbol{r})\right] \quad (2)$$

Bold variables are vector quantities and $d = |\boldsymbol{r} - \boldsymbol{e}|$ (Brody et al., 1973).

### 2.5. Implementing a temporal constraint

Many source localization procedures impose a variety of constraints on the dipole solutions which make use of known cortical anatomy or limit the time-window of interest (Scherg and Berg, 1991; Dale and Sereno, 1993; Clark and Hillyard, 1996). Such constraints increase the accuracy of the results by judiciously reducing the solution space. It is reasonable to assume that the dipole orientation of a cortical source is independent of time; in other words, the dipole orientation is stationary and only the dipole magnitude changes in time (Scherg and Berg, 1991).

$$\boldsymbol{M}(p,t) = \boldsymbol{M}(p)T\ (p,t) \quad \text{where } \Sigma T(p,t)^2 = 1 \quad (3)$$

We further assume that each group of stimulus patches at the same eccentricity, defining an annulus, generate source responses with similar temporal waveforms, T($t$) (Baseler and Sutter, 1997; Carney et al., 1998).

$$T(p,t) = \mathrm{T}(t) \text{ where } \Sigma T(t)^2 = 1 \quad (4)$$

Thus Eq. (1) becomes

$$V_{fit}(\boldsymbol{e},p,t) = \boldsymbol{W}(\boldsymbol{e},\boldsymbol{r}(p))\cdot\boldsymbol{M}(p)T(t) \quad (5)$$

where the inner product $\boldsymbol{W}\cdot\boldsymbol{M}$ is the magnitude of the surface potential and T($t$) describes its temporal modulation.

### 2.6. Warping electrode locations

Actual electrode locations were projected onto a unit sphere to accommodate the spherical head model used in the source localization procedure. The locations were determined using a Polhemus 3D digitizer. The best fitting radius and center were obtained by minimizing the difference between the actual and spherical electrode locations using the Marquardt least-squares algorithm.

### 2.7. Verification

The most common technique to determine the validity of a solution is to compare the resulting dipole locations with the known locations of the multiple visual areas (Ossenblok and Spekreijse, 1991; Plendl et al., 1993; Gonzalez et al., 1994). An even more detailed method of verification is based upon the known retinotopic configuration within early visual areas. This method has been used to verify localization results in primary visual cortex with 7 or 6 stimulus locations (Aine et al., 1996; Gevins, 1996). Information about the orientation of the cortical surface can be useful in verifying the source localization results as well. Striate cortex is known to follow the calcarine sulcus. At a given eccentricity, a stimulus patch in the upper visual field and a stimulus patch in the lower visual field are expected to activate the lower and upper bank of the calcarine sulcus respectively. The corresponding dipoles are expected to reverse in polarity. This reversal is characteristic of the primary visual cortex and serves as a means to identify signals from this source.

Dipoles within an annulus are expected to show continuity of location. In addition, results across annuli should show continuity in location, magnitude, and temporal response characteristics. Since results are obtained independently between annuli, these continuity checks provide a powerful means of validating this procedure.

## 3. Results and discussion

The numbering scheme of the stimulus patches is given in Fig. 4. One annulus of patches is shown in Fig. 5a and the corresponding classical V1 projection is shown in Fig. 5b (Horton and Hoyt, 1991a). In standard source localization, a separate time function is assumed for every dipole response to each stimulus patch (where $T$ is a function of both $p$ and $t$). Using standard source localization, Fig. 6 shows the time-functions for dipoles within annulus two for subject HB. The similarity of these time-functions gives support to the previous supposition that dipoles generated by patches at a

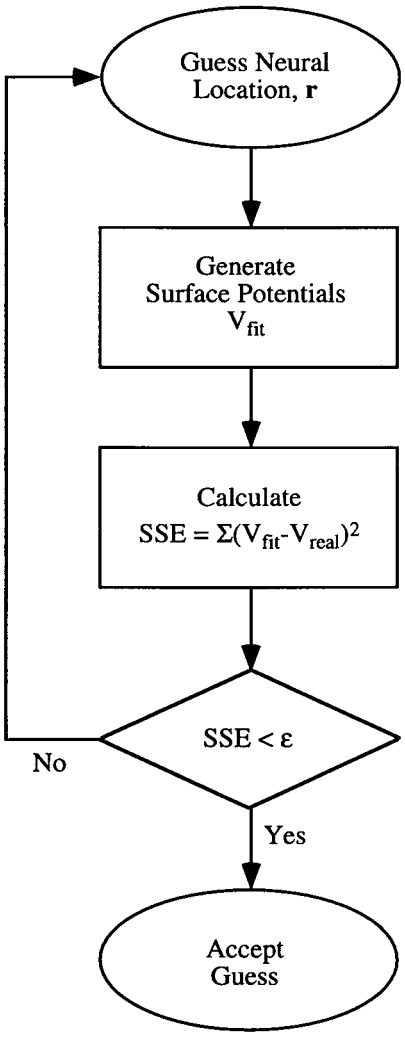


Fig. 3. Flow chart of the iterative procedure used to determine dipole location given a topographic voltage distribution. The first step was to guess the location and magnitude of the underlying neural activity. For each stimulus patch, this was done by a search using a 3 × 3 grid contralateral to the stimulus. A radial dipole at a depth of 0.7 (where 1 is the radius of the head) was randomly placed on one of the grid points. Linear regression was used to obtain the initial guess for the timecourse. Identical results were obtained regardless of the initial parameter values. For each loop through the iteration, a model of the head and brain activity was used to generate a voltage distribution, $V_{fit}$ (see Eqs. (1) and (2) in the text). The difference between $V_{fit}$ and $V_{real}$ contribute to an error term. The sum of squared error, SSE, is calculated by summing the square of this error term over all electrodes and all time-points. SSE is minimized using the Marquardt least-squares analysis with 3 parameters (3 for location with linear regression for magnitude inside the least-squares routine and linear time-course regression outside the least-squares routine). If the change in SSE from one iteration to the next is below a certain tolerance level, ϵ, then the guess of the neural location is accepted. If it is not, then a new guess is used and the process repeats until the SSE stabilizes.

similar eccentricity have similar time-functions (justifying the use of the common-time function assumption, Eq. 4).

Fig. 7 shows the dipole solutions for annulus 5 with and without the temporal constraint for subject TC. Although most of the dipole locations and magnitudes are similar,

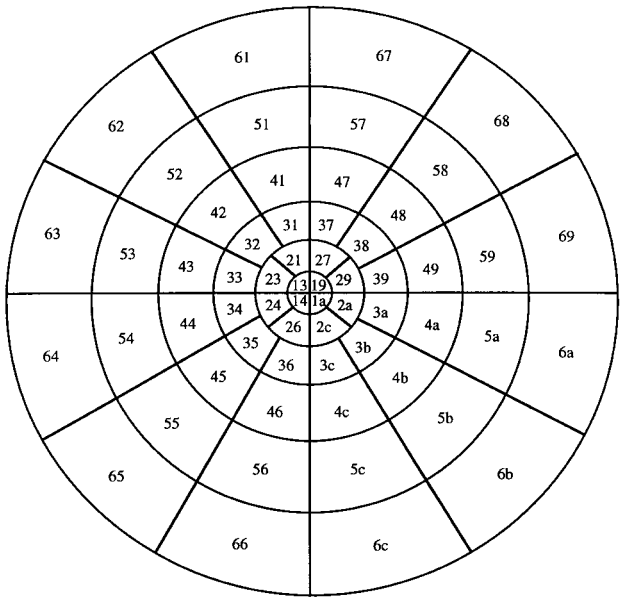


Fig. 4. Stimulus patch numbering scheme. Patches of similar eccentricity within an annulus have the same prefix which increases sequentially from the center toward the periphery. The suffix in each semi-annulus is labeled sequentially from top to bottom starting from 1 to 6 on the left and from 7 to c on the right. In the two central annuli, the suffix is labeled in a way to make the patches adjacent to the horizontal and vertical meridian consistent across annuli.

the dipole solutions of patches 57, 5b, and 54 in Fig. 7a, without the temporal constraint, and Fig. 7b, with the temporal constraint, were quite different. The solutions to patches 57 and 5b without the temporal constraint are located on the ipsilateral side of the head and with the temporal constraint are located on the expected contralateral side of the head. The solution to patch 5b with the temporal constraint is more continuous with surrounding patches 5a and 5c as expected from the retinotopic organization of V1. A possible explanation for the aberrant solution of patch 5b without the temporal constraint is that the source is located near the base of the calcarine sulcus where the activity of two opposing faces of cortex nearly cancel.

Fig. 8 shows that cancellation may indeed be the cause.

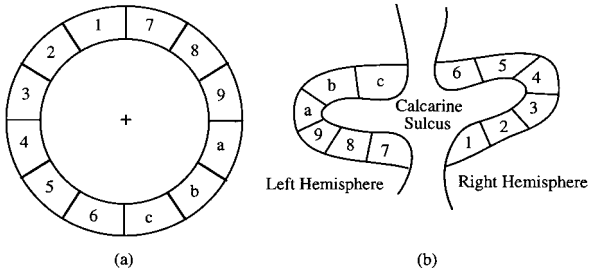


Fig. 5. (a) Patches within one annulus and (b) an idealized representation of each patch's representation in a posterior view of primary visual cortex (coronal slice through the occipital cortex). Stimuli are mapped onto the contralateral hemisphere and inverted on the primary visual cortex surrounding the calcarine sulcus.

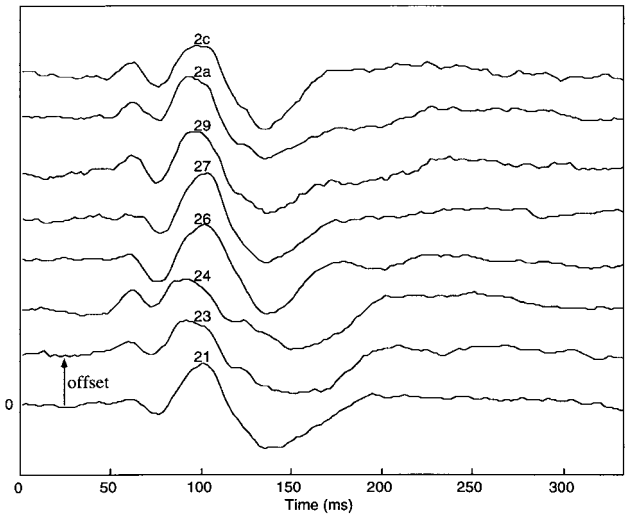


Fig. 6. Single dipole time-courses for all patches in annulus 2 for subject HB. Responses are offset by the amount shown (offset arrow) to simplify waveform comparisons. Time-functions are normalized to unity since it is the dipole magnitude that carries the information about the size of the response. Magnitudes are allowed to vary across patches within an annulus.

From the raw surface VEP's it is evident that moving from patch 5a to 5b to 5c involves a polarity inversion of the principal response component and its apparent cancellation in patch 5b. A similar effect of cancellation and polarity inversion is also evident for the 53 to 54 to 55 sequence of patches shown in Fig. 8b.

In the absence of a strong striate signal for patches 5b and 54, it is not surprising that standard DSL methods result in dipole locations that lack continuity with neighboring locations. The identified source may reflect fitting a dipole to extrastriate sources or background noise. By using the common time function assumption, the analyses focuses on that part of the temporal signal that matches the striate signal of the surrounding sources, thereby achieving much better source localization even for patches with weak self-canceling sources. We see this effect for sources 5b and 54 in Fig. 7. When the common time function assumption is applied (Fig. 7b), the sources move to locations that are continuous with respect to neighboring source solutions.

The average percent variance accounted for by a one dipole fit with the time-function constraint (conducted independently for each annulus and then averaged), was found to be 52% for subject TC, 51% for subject HB, and 39% for subject SD. There are 115 200 data points (200 time points X 48 electrodes X 12 patches) which are fit by 271 parameters ((3 for location + 3 for magnitude) X 12 patches + 199 for time) in the one dipole fit procedure for each of the outer 4 annuli. Considering the simplicity of the model, which constitutes a 425/1 data reduction, and the noisiness of the data, the percentage variance accounted for suggests that the response is dominated by a single neural generator. The percentage variance accounted for also provides additional support that our time function assumption is correct

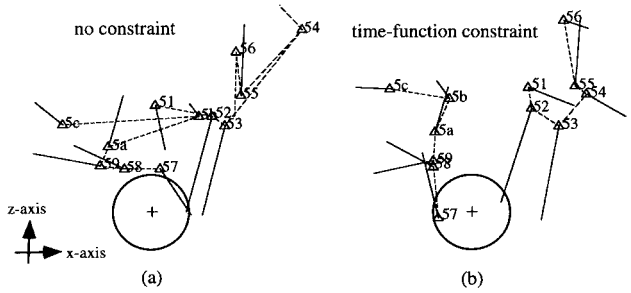


Fig. 7. Single dipole locations and magnitudes in annulus 5 for subject TC with (a) standard source localization (no common time-function) and (b) source localization using the common time-function constraint.

otherwise the percentage variance accounted for would be much lower.

The waveform reversals in Fig. 8 support the conjecture that the dominant source is generated by primary visual cortex. The activity of different peaks within these types of waveforms have been analyzed extensively in a number of studies (Mangun et al., 1993; Gonzalez et al., 1994; Clark et al., 1995). The first peak elicited by a checkerboard flash stimulus is typically attributed to visual area V1 because this peak reverses in polarity as the stimulus position is changed from the upper to lower visual field (resulting in activity on the lower and upper bank of the calcarine sulcus). Clark et al. (1995) showed that the peaks which follow the first component in response to a checkerboard flash stimulus do not reverse in polarity and are, therefore, attributed to extrastriate cortex. This constancy in waveform polarity is due to the topology in the cortical organization of extrastriate visual areas. Additionally, sources generated in visual areas V2 and V3 are not continuous in cortical representation as stimulation progresses across the horizontal meridian but rather jump discontinuously across cortex (Horton and Hoyt, 199lb). If waveforms and dipole sources are shown to reverse in polarity and maintain continuity across the horizontal meridian, the

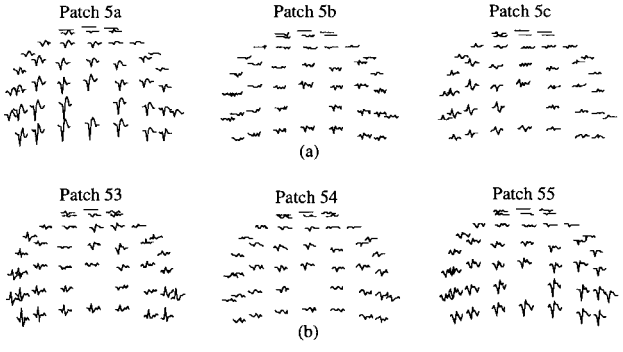


Fig. 8. VEP responses placed at the location of each recording electrode (as viewed from the posterior) for subject TC due to stimulation by (a) adjacent patches 5a, 5b, and 5c and by (b) adjacent patches 53, 54, 55. Epoch ranges from 0 to 333 ms for all electrodes with a peak-to-peak amplitude in the 300 nanovolt range. The response at oz is missing due to an intermittent connection.

underlying neural generators likely represent activity of primary visual cortex. As polarity reversals and continuity across the horizontal meridian are consistent across all subjects (see Fig. 9), this lends support to the assertion that V1 is responsible for the dominant response when using our multi-stimulus checkerboard array.

Fig. 9 shows the one dipole solutions corresponding to each stimulus patch in the multi-stimulus array obtained for all subjects. The common time-function constraint was implemented within each annulus. A number of consistencies with the known cortical organization of primary visual cortex can be observed in this figure: stimulus location suffixes are numbered from 1 to 6 from top-to-bottom on the left and from 7 to c from top-to-bottom on the right. Contralateral activation can be verified by observing that all neural solutions on the left were stimulated by patches on the right (suffixes from 7 to c) and all neural solutions on the right were stimulated by patches on the left (suffixes from 1 to 6). Field inversion can also be observed since the lower suffix numbers at the top of the stimulus are nearer the bottom of the brain. This contralateral and inverted retinotopic organization was obtained for all subjects.

In addition to retinotopy, within hemispheric similarities and inter-hemispheric differences can also be observed in the solutions. For example, dipole locations on the right side of the head of subject TC show a curvature that is not apparent on the left.

### 3.1. Cortical mapping

An appropriate 3-D retinotopic map of primary visual cortex can be reconstructed from the dipole locations and magnitudes. Fig. 10 displays a partial cortical map corresponding to stimuli in the upper left quadrant of the visual field for subject TC. In the interest of mapping the lower bank of the right primary visual cortex, stimuli from annuli 3–6 with suffixes 2 and 3 were selected. Fig. 10a shows that all dipole orientations are pointing in similar directions as expected from a roughly planar region of cortex. Fig. l0b illustrates that stimuli at increasing eccentricity are mapped more anterior in the cortex. Both of these results correspond well with the known cortical architecture of V1.

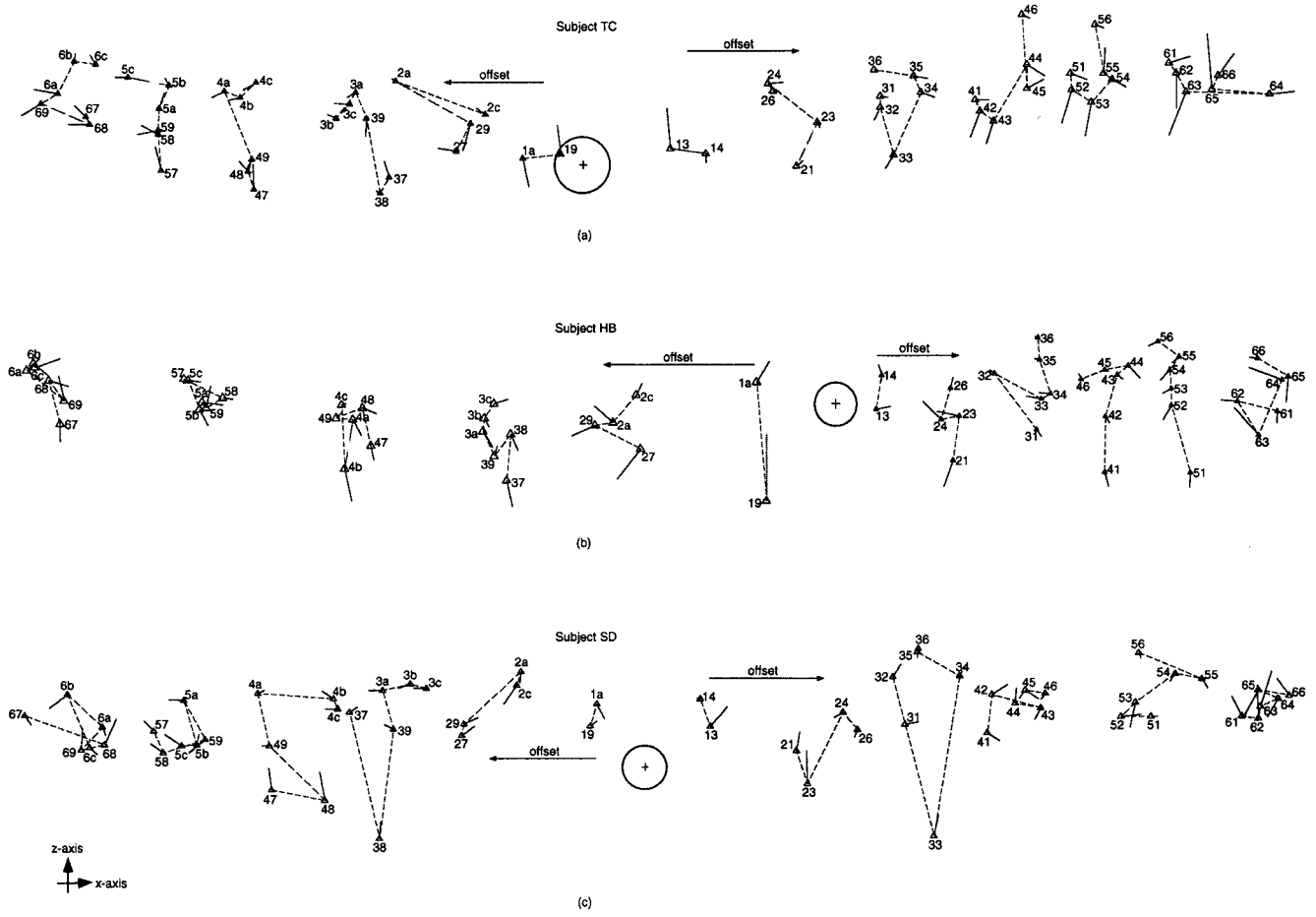


Fig. 9. Back of the head view of all dipole solutions for all subjects. Dipoles generated from patches in the center annuli are at their actual position and successive semi-annuli are offset in either direction by the amount shown (offset arrow). The center of the head is labeled with a + and a 1 cm radius circle is placed around the center as a reference. Solutions within a hemisphere semi-annulus are connected by dotted lines and should approximate the location of the cortex between the localized patches.

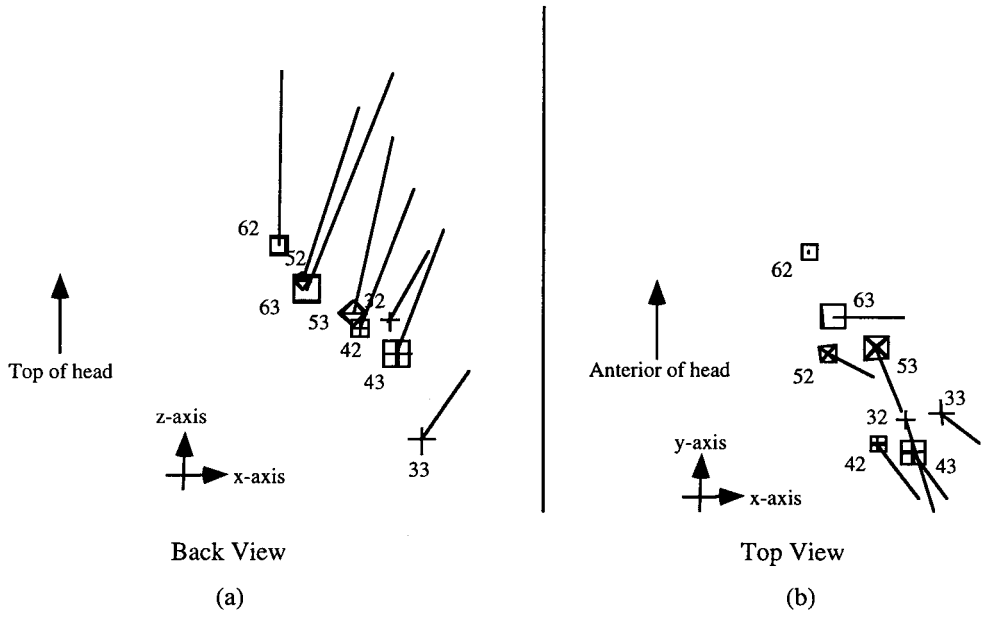


Fig. 10. Dipole locations and magnitudes for a radial wedge of patches including 32, 33, 42, 43, 52, 53, 62, and 63 from the (a) back view and (b) top view. Subject TC.

## 4. General discussion

The waveform polarity reversals (Clark et al., 1995), the dipole retinotopic organization (Horton and Hoyt, 1991a), and continuity across the horizontal meridian (Horton and Hoyt, 1991b) all indicate that this method of stimulation and analysis reveals primary visual cortex activation.

The assumption that the dipoles generated by patches in an annulus had the same temporal waveform assisted in localizing weaker sources. In the case of a weak V1 source (due to the source lying in a cortical fold), a dipole solution would be noise or a non-striate source and would not conform to fit to a smooth transition across V1. By forcing the time-functions of all dipoles corresponding to a given annulus to be the same, the aberrant dipoles were localized closer to their expected locations (see Fig. 7). Still, if the signal strength of V1 is too low, the solutions will not be 'rescued'. These regions can be found by inspecting the dipole solutions and observing an incoherent or inconsistent set of results. The location accuracy of such dipoles should not be trusted.

Some groups have implemented a symmetry constraint between hemispheres when conducting source localization of higher cortical regions (Scherg and Berg, 1991; Plendl et al., 1993; Gonzalez et al., 1994; Clark and Hillyard, 1996). Our results indicate that there are large interhemispheric differences in primary visual cortex that likely exist in higher visual areas. Therefore, the accuracy of dipole solutions obtained using the symmetry constraint must be reconsidered.

Before the present study, the most detailed retinotopic map of human visual area V1 with high temporal resolution was generated using 7 different stimulus locations (Aine et al., 1996). Our method has provided a detailed retinotopic map with nearly 10 times as many stimuli. In the future, the high temporal resolution of the retinotopic information gained with this method may be coupled with the results of fMRI. As the VEP results using this method are likely to be locally coherent but globally inaccurate (showing local continuity, but shifted due to the poor head model), an algorithm will be developed to warp our locations and magnitudes onto the retinotopic map provided by fMRI.

Given a typical visual stimulus, many visual areas are activated to process different stimulus attributes like shape, color, and motion. Therefore, the study of simultaneously active visual areas is crucial in understanding how we process information in the normal visual environment. To emphasize response components from extrastriate areas, the properties of the stimulus array may be altered. The temporal constraint is expected to dramatically increase the accuracy of extrastriate source localization. By comparing the time course of activation in each visual area, this method may be capable of realizing the interplay between them. By combining this information with retinotopic maps provided by fMRI, this technique has the potential of providing detailed temporal and spatial information about the cortical dynamics of early visual areas.

## References

Aine CJ, Supek S, George JS, Ranken D, Lewine J, Sanders J, Best E, Tiee W, Flynn ER, Wood CC. Retinotopic organization of human visual cortex: departures from the classical model. Cerebral Cortex 1996;6:354–361.

Baseler HA, Sutter EE. M and P Components of the VEP and their visual field distribution. Vision Res 1997;37:675–690.

Baseler HA, Sutter EE, Klein SA, Carney T. The topography of visual evoked response properties across the visual field. Electroenceph clin Neurophysiol 1994;90:65–81.

Brody DA, Terry FH, Ideker RE. Eccentric dipole in a spherical medium: generalized expression for surface potentials. IEEE Trans Biomed Eng 1973;20:141–143.

Carney T, Slotnick SD, Klein SA, Dastmalchi S. Localization of VEP sources using a common time function. Poster presented at the Association for Research in Vision and Opthalmology Conference, 1998;S182.

Clark VP, Hillyard SA. Spatial selective attention affects early extrastriate but not striate components of the visual evoked potential. J Cog Neurosci 1996;8:387–402.

Clark VP, Fan S, Hillyard SA. Identification of early visual evoked potential generators by retinotopic and topographic analysis. Human Brain Mapping 1995;2:170–187.

Dale AM, Sereno MI. Improved localization of cortical activity by combining EEG and MEG with MRI cortical surface reconstruction: a linear approach. J Cog Neurosci 1993;5:162–176.

DeYoe EA, Carman GJ, Bandettini P, Glickman S, Wieser J, Cox R, Miller D, Neitz J. Mapping striate and extrastriate visual areas in human cerebral cortex. Proc Nat Acad Sci USA 1996;93:2382–2386.

Engel SA, Glover GH, Wandell BA. Retinotopic organization in human visual cortex and the spatial precision of functional MRI. Cerebral Cortex 1997;7:181–192.

Gevins A. High resolution evoked potentials of cognition. Brain Topography 1996;8:189–199.

Gonzalez CMG, Clark VP, Fan S, Luck SJ, Hillyard SA. Sources of attention-sensitive visual event-related potentials. Brain Topography 1994;7:41–51.

Holmes G. The organization of the visual cortex in man. Proceedings of the Royal Society of London (Biological) 1945;132:348–361.

Horton JC, Hoyt WF. The representation of the visual field in human striate cortex. A revision of the classic Holmes map. Arch Opthalmol 1991;109:816–824.

Horton JC, Hoyt WF. Quadrantic visual field defects. A hallmark of lesions in extrastriate (V2/V3) cortex. Brain 1991;114:1703–1718.

Jasper HH. Appendix to report to Committee on Clinical Examination in EEG: the ten-twenty electrode system of International Federation. Electroenceph clin Neurophysiol 1958;10:371–375.

Mangun GR, Hillyard SA, Luck SJ. Electro-cortical substrates of visual selective attention. In: Meyer DE, Komblum S, editors. Attention and Performance XIV, MA: Cambridge MIT Press, 1993.

Ossenblok P, Spekreijse H. The extrastriate generators of the EP to checkerboard onset. A source localization approach. Electroenceph clin Neurophysiol 1991;80:181–193.

Plendl H, Paulus W, Roberts IG, Botzel K, Towell A, Pitman JR, Scherg M, Halliday AM. The time course and location of cerebral evoked activity associated with the processing of colour stimuli in man. Neurosci Lett 1993;150:9–12.

Scherg M, Berg P. Use of prior knowledge in brain electromagnetic source analysis. Brain Topography 1991;4:143–150.

Schiefer U, Skalej M, Kolb R, Grodd W, Fahle M, Herzog H. Cerebral activity during visual stimulation - a positron emission tomography and functional magnetic resonance imaging study. German J Ophthalmol 1996;5:109–117.

Schiefer U, Skalej M, Kolb M, Dietrich TJ, Kolb R, Braun C, Peterson D. Lesion location influences perception of homonymous scotoma during flickering random dot pattern stimulation. Vision Research 1998;38:1301–1312.

Sereno MI, McDonald CT, Allman JM. Analysis of retinotopic maps in extrastriate cortex. Cerebral Cortex 1994;4:601–620.

Skalej M, Schiefer U, Nagele T, Grodd W, Voigt K. Funktionelle Bildgebund des visuellen Kortex mit der MRT. Klinische Neuroradiologie 1995;5:176–183.

Spalding JMD. Wounds of the visual pathway. II. The striate cortex. J Neurol Neurosurg Psychol 1952;15:169–183.

Sutter EE, Tran D. The field topography of ERG components in man I. The photopic luminance response. Vision Research 1992;32:433–446.

Sutter EE. Deterministic approach to nonlinear systems analysis. In: Pinter RB, Nabet B, editors. Nonlinear vision, Boca Raton: CRC Press, 1992. pp. 171–220.